Exceptionally bright TeV flares from the binary LS I +61° 303

Anna OFdB[1], Andy Smith[2], VERITAS Collaboration[3]

ABSTRACT

The TeV binary system LS I +61° 303 is known for its regular, non-thermal emission pattern which traces the orbital period of the compact object in its 26.5 day orbit around its B0 Ve star companion. When active in the TeV regime, the system typically presents elevated emission around apastron passage with flux levels between 5 and 15 % of the steady flux from the Crab Nebula (> 300 GeV). In this article, VERITAS observations of LS I +61° 303 taken in late 2014 are presented, during which bright TeV flares around apastron at flux levels peaking above 30% of the Crab Nebula flux were detected. This is the brightest such activity from this source ever seen in the TeV regime. The strong outbursts have rise and fall times of less than a day. The short timescale of the flares, in conjunction with the observation of 10 TeV photons from LS I +61° 303 during the flares, provides constraints on the nature and efficiency of the accelerating mechanism in the source.

Subject headings:

1. Introduction

High-mass X-ray binaries (HMXBs) are a class of binary system that consist of a compact object (either a black hole or a neutron star) and a massive stellar companion, and emit in X-rays. The current generation of imaging atmospheric-Cherenkov telescopes (IACTs) has facilitated the study of HMXBs which exhibit TeV emission. The class of TeV binaries is quite sparse, consisting of only a handful of sources: LS 5039 (Aharonian et al. 2005b), PSR B1259-63 (Aharonian et al. 2005a), LS I +61° 303 (Albert et al. 2006), HESS J0632+057 (Aharonian et al. 2007), 1FGL J1018.6-5856 (Abramowski et al. 2015), and the newest member of the class, TeV 2032+413 (Lyne et al. 2015). Of these, only the compact objects of PSR B1259-63 and TeV 2032+413 have been firmly identified as pulsars. There is still a large degree of ambiguity concerning the nature of the compact object within the other systems. Consequently, the fundamental mechanism responsible for the TeV emission along with its characteristic variability on the timescale of one orbital period remains uncertain.

The orbital periods of TeV-emitting HMXBs vary from several days (LS 5039) to many years (TeV 2032+413). As the TeV emission varies strongly as a function of the orbital phase, the various sources may only have short windows during which they can be detected and studied in the TeV regime. Of the TeV binaries, LS I +61° 303 is the only known source in the Northern Hemisphere that has a short enough orbital period (26.5 days) to allow for regular study with TeV instruments.

Located at a distance of ~2 kpc (Frail & Hjellming 1991), LS I +61° 303 is composed of a B0 Ve star and a compact object (Hutchings & Crampton 1981; Casares et al. 2005). The observed multiwavelength emission is variable at all energies and modulated with a period of $P \approx 26.5$ days, believed to be associated with the orbital motion of the binary system (Albert et al. 2006; Esposito et al. 2007; Acciari et al. 2008; Abdo et al. 2009; Li et al. 2012; Massi et al. 2015). Radial velocity measurements show the orbit to be elliptical with eccentricity $e = 0.537 \pm 0.034$, with periastron occurring around phase $\phi = 0.275$, apastron at $\phi = 0.775$, superior conjunction at $\phi = 0.081$

[1]Germany

[2]America

[3]Everywhere

and inferior conjunction at $\phi = 0.313$ (Aragona et al. 2009). The periastron distance between the star and the compact object is estimated at 2.84×10^{12} cm (0.19 AU) and the apastron distance at 9.57×10^{12} cm (0.64 AU) (Dubus 2013). However, the inclination of the system is not exactly known but is expected to lie in the range $10° - 60°$ according to Casares et al. (2005), leading to some uncertainty in the orbital parameters.

In this work, we present the results of the VERITAS campaign on LS I +61° 303 in October – December of 2014. During this time, VERITAS observed historically bright flares from LS I +61° 303 around apastron, with the source exhibiting flux levels a factor of 2 – 3 times higher than ever observed.

2. Observations

The VERITAS IACT array, located at the base of Mt. Hopkins, AZ (1.3 km a.s.l., 31°40′ N, 110°57′ W) consists of four 12 m diameter Davies-Cotton design optical telescopes. VERITAS is sensitive to photons with energies from 85 GeV to 30 TeV and has the ability to detect a 1 % Crab Nebula source in approximately 25 hours[1]. For a full description of the hardware components and analysis methods utilized by VERITAS, see Holder et al. (2008); Kieda, D. (2013); Acciari et al. (2008), and references therein.

In the 2014 season, VERITAS observations of LS I +61° 303 were taken from October 16 (MJD 56946) to December 12 (MJD 57003), comprising a total of 24.7 hours of quality-selected livetime. These observations sampled three separate orbital periods, covering the orbital phase regions of $\phi = 0.5 - 0.2$ (see Figure 1 and Table 1). Over the entire set of observations, a total of 449 excess events above an energy threshold of 300 GeV were detected above background. This is equivalent to a statistical significance of 21 standard deviations (21σ, calculated using Equation 17 of Li & Ma 1983).

During the first orbit observed (in October), the source presented the largest of its flares (hereafter "F1"), beginning on 2014 October 17 (MJD 56947, $\phi = 0.55$). The emission reached a peak flux of $(3.20 \pm 0.34) \times 10^{-11}$ cm^{-2} s^{-1} above 300 GeV on

[1] http://veritas.sao.arizona.edu/specifications

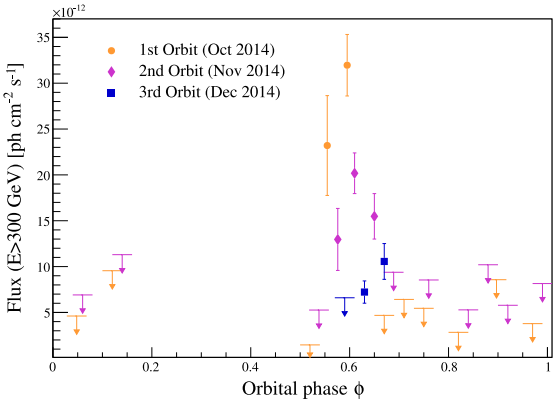

Fig. 1.— Light curve of LS I +61° 303 during the 2014 observation season shown as a function of orbital phase in nightly bins. The data for the first orbit (October) are shown with orange circles, while the second orbit (November) is represented by purple diamonds, and the third (December) by blue squares. Flux upper limits at the 99% confidence level (using the unbounded approach of Rolke et al. 2005) are shown for points with significance $< 3\,\sigma$ and are represented by arrows.

October 18 (MJD 56948, $\phi = 0.60$). This flare reached a peak flux of approximately 30% of the Crab Nebula flux above the same energy threshold, representing the largest flux ever detected from the source. Unfortunately, observations were limited by poor weather conditions the following two nights and only recommenced on October 20 (MJD 56950), by which time the flux from the source had already decreased. During the second orbital passage in November, VERITAS detected another period of elevated flux ("F2") from the source at similar orbital phases ($\phi = 0.55 - 0.65$) with peak emission of $(2.02 \pm 0.22) \times 10^{-11}$ cm^{-2} s^{-1} on November 14 (MJD 56975, $\phi = 0.61$).

The rise and fall times of the flares were determined by fitting the following function (Abdo et al. 2010, Equation 7) to the light curve of each orbit:

$$F(t) = F_c + F_0 \left(e^{\frac{t_0 - t}{t_r}} + e^{\frac{t - t_0}{t_f}} \right), \qquad (1)$$

where F_c is an assumed constant level underlying the flare, F_0 is a measure of the amplitude of the flare, t_0 is approximately the time of the peak of the flare, and t_r and t_f are the rise and

TABLE 1
VERITAS OBSERVATIONS OF LS I +61° 303 IN 2014

Date observed [MJD]	Orbital phase (ϕ)	Flux($> 300\,\mathrm{GeV}$) [$\times 10^{-11}$ cm^{-2} s^{-1}]
56946.3	0.52	<0.15
56947.3	0.55	2.32 ± 0.54
56948.3	0.60	3.20 ± 0.34
56950.0	0.67	<0.47
56951.0	0.71	<0.64
56952.0	0.75	<0.55
56954.0	0.82	<0.28
56956.0	0.90	<0.86
56958.0	0.97	<0.38
56960.0	0.05	<0.46
56962.0	0.12	<0.96
56973.0	0.54	<0.53
56974.0	0.58	1.30 ± 0.34
56975.0	0.61	2.02 ± 0.22
56976.0	0.65	1.55 ± 0.25
56977.0	0.69	<0.94
56979.0	0.76	<0.85
56981.0	0.84	<0.53
56982.0	0.88	<1.02
56983.0	0.92	<0.58
56985.0	0.99	<0.82
56987.0	0.06	<0.69
56989.0	0.14	<1.13
57001.0	0.59	<0.66
57002.0	0.63	0.72 ± 0.12
57003.0	0.67	1.06 ± 0.20

fall time, respectively. The parameter t_0 is fixed to the MJD of the observed peak during the fit. The fit to the first orbit has poor fit probability of $P = 3 \times 10^{-7}$ (χ^2/NDF = 43.6/7). The second orbit is well fit by this function, with a fit probability of 10^{-1} (χ^2/NDF = 13.1/8), possibly due to the better data sampling throughout this flare. The rise and fall times of F2 are found to be 0.65 ± 0.13 days and 0.83 ± 0.12 days, respectively. The flares were also fitted with a piecewise-defined exponential function of the form

$$F(t) = \begin{cases} F_0 e^{-\frac{|t-t_0|}{t_r}}, & t < t_0 \\ F_0 e^{-\frac{|t-t_0|}{t_f}}, & t \geq t_0 \end{cases} . \quad (2)$$

However, poor fit probabilities of 10^{-7} and 3×10^{-19} were obtained for F1 and F2, respectively.

Over the complete time range of these observations, variability on a nightly timescale was tested using the method described in Aliu et al. (2013). Similar to their findings for this source, a marginal indication of nightly variability at a significance level of $\sim 3\,\sigma$ post trials was found in F1.

Follow-up observations conducted by VERITAS during the next month (December) covered the orbital phases of $\phi = 0.59 - 0.67$ and detected the source at a lower flux level. The previous flares in 2014 were detected at $\phi \simeq 0.60$, but during this cycle the source reached only $(0.72 \pm 0.12) \times 10^{-11}$ cm^{-2} s^{-1} at a comparable orbital phase on December 11 (MJD 57002, $\phi = 0.63$). The peak emission of this cycle occurred on the following night at an orbital phase of $\phi = 0.67$. The observations during this month seem to exclude the type of peaked flaring behavior seen at the same phase range in the previous two orbital cycles, perhaps indicating some orbit-to-orbit variations in the source.

The average differential energy spectrum from all observations of LS I +61° 303 during the 2014 observing season is well fit with a power law of the form

$$\frac{dN}{dE} = N_0 \left(\frac{E}{1\,\mathrm{TeV}} \right)^{\Gamma} , \quad (3)$$

in which N_0 is the normalization at the pivot energy of 1 TeV, and Γ is the spectral index. The measured parameters are consistent with past observations. Differential energy spectra were also extracted from F1 (October 17 – 18) and F2 (November 13 – 15) and show a similar spectral shape, albeit with a higher normalization constant. The parameters from the spectral fits are given in Table 2. An uncertainty on the energy scale of 15 – 25% results in a systematic uncertainty of $\sim$ 20% on the flux normalization and $\sim$ 40% on the integral flux, assuming a spectral index of -2.35. The systematic uncertainty on the spectral index is estimated at $\sim$ 0.3, accounting for uncertainties on the collection efficiency, sky brightness, analysis cuts and simulation model. All spectra are shown in Figure 2 along with previous spectral measurements (Acciari et al. 2008; Aleksic et al. 2012) for comparison.

The highest energy gamma-ray candidates observed were detected during the peak night of F1 with an energy of ~10 TeV. There are no events in the OFF region with energies above 4 TeV on this night, so it is assumed that the contribution of the background at ~10 TeV is negligible.

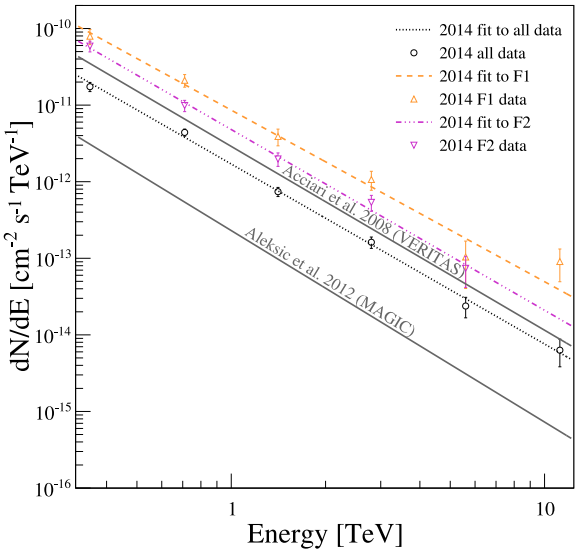

Fig. 2.— Average and flare differential energy spectra of LS I +61° 303 from the VERITAS 2014 observations, shown in comparison with the average spectra from Acciari et al. (2008) and Aleksic et al. (2012).

During these observations, the source was also monitored by the *Fermi*-LAT (0.1 – 300 GeV), the *Swift*-XRT (0.2 – 10 keV), and both the RATAN and AMI radio instruments (4/6 – 15 GHz). In ad-

TABLE 2
SPECTRAL PARAMETERS OF THE POWER LAW FITS TO THE OBSERVATIONS OF LS I +61° 303 IN THE ENERGY RANGE 0.3 – 20 TEV.

Observations	Normalization [$\times 10^{-12}$ cm^{-2} s^{-1} TeV^{-1}]	Spectral index
All (average)	$1.7 \pm 0.7_{\rm stat} \pm 0.9_{\rm sys}$	$-2.35 \pm 0.32_{\rm stat} \pm 0.3_{\rm sys}$
F1 (Oct 17 – 18)	$8.6 \pm 1.0_{\rm stat} \pm 4.3_{\rm sys}$	$-2.24 \pm 0.12_{\rm stat} \pm 0.3_{\rm sys}$
F2 (Nov 13 – 15)	$4.8 \pm 0.4_{\rm stat} \pm 2.4_{\rm sys}$	$-2.36 \pm 0.12_{\rm stat} \pm 0.3_{\rm sys}$

dition, Hα monitoring of the system took place at the Ritter Observatory in Toledo, Ohio (USA). After F2 was detected by VERITAS, an Astronomer's Telegram[2] (Holder 2015) was released, notifying the astronomical community of the historic flux levels and triggering more intense observations by multiwavelength partners, as well as additional observations with the MAGIC TeV observatory. The results of this multiwavelength campaign are under analysis and will be presented in an upcoming publication.

3. Discussion and Conclusion

The nature of the compact object in LS I +61° 303 is not firmly established and, as a result, proposed emission mechanisms for the system cover a range of possibilities. These mechanisms fall into two main categories: microquasar (μQ) and pulsar binary (PB). In the μQ scenario, non-thermal particle-acceleration processes occur in the jet of an accreting compact object (Massi et al. 2001; Massi & Jaron 2013; Massi et al. 2015), whereas the binary pulsar scenario utilizes the presence of a shocked wind in which particle acceleration is the result of the interaction between the stellar and the pulsar winds (Dhawan et al. 2006). While some versions of both models utilize a hadronic primary population, the majority of both model types employ leptonic origins for the observed non-thermal emission.

In a leptonic scenario, the TeV emission is the result of inverse-Compton (IC) scattering of electrons accelerated in the jet (μQ) or at the shock front (PB). Regardless of the primary mechanism of generation, Khangulyan et al. (2008) provide a prescription to calculate model-independent limits on the magnetic field strength and the efficiency of the accelerator within an IC scenario. Given the temperature $T = 2.25 \times 10^4$ K (Dubus 2013) of the B0 Ve star in LS I +61° 303, the average energy of the stellar photons is $3kT \approx 6$ eV, and the IC scattering will take place deep in the Klein–Nishina regime, in which almost all of the electron energy is transferred to the scattered photons. Thus, the presence of ~10 TeV photons requires ~10 TeV electrons in the emitter, as well as forcing the acceleration time to be less than the cooling time. Following the calculations of Khangulyan et al. (2008), the acceleration timescale of the electrons can be expressed as

$$t_{\rm acc} = \eta_{\rm acc} r_{\rm L} c^{-1} \approx 0.1 \eta_{\rm acc} E_{\rm TeV} B_{\rm G}^{-1} \, {\rm s}, \quad (4)$$

where $r_{\rm L}$ is the Larmor radius of the electron, $E_{\rm TeV}$ is the energy of the electron in units of TeV, $B_{\rm G}$ is the magnetic field strength in units of Gauss, and $\eta_{\rm acc} > 1$ is a parameter describing the efficiency of the accelerator (in general $\eta_{\rm acc} \gg 1$). The characteristic cooling time of electrons in the Klein–Nishina regime is given by

$$t_{\rm KN} \approx 10^3 d_{13}^2 E_{\rm TeV}^{0.7} \, {\rm s}, \quad (5)$$

where d_{13} is the distance between the emitter and the optical star in units of 10^{13} cm, and the synchrotron cooling time is

$$t_{\rm sy} \approx 4 \times 10^2 B_{\rm G}^{-2} E_{\rm TeV}^{-1} \, {\rm s}. \quad (6)$$

The relation $t_{\rm KN} < t_{\rm sy}$ can also be set due to the fact that IC losses in the Klein-Nishina regime allow for the hard electron spectra (harder than -2) necessary to produce hard gamma-ray spectral indices (from -2 to -2.5). Thus, the magnetic field in the emitter is constrained by the relation

$$B < 0.6 d_{13}^{-1} E_{\rm TeV}^{-0.85} \ {\rm G}. \quad (7)$$

[2] www.astronomerstelegram.org

Using $E_{\rm TeV} = 10$, as measured during F1, gives values of $B \lesssim 0.3\,{\rm G}$ at periastron and $B \lesssim 0.1\,{\rm G}$ at apastron, assuming that the emitter is located close to the compact object.

As the cooling time is dominated by $t_{\rm KN}$, the requirement that the acceleration time is less than the cooling time yields the relation $t_{\rm acc} < t_{\rm KN}$ which gives

$$B > 10^{-4} d_{13}^{-2} E_{\rm TeV}^{0.3} \eta_{\rm acc}\ {\rm G}. \quad (8)$$

This gives values of $B \gtrsim (2.5 \times 10^{-3})\eta_{\rm acc}$ G at periastron and $B \gtrsim (2.2 \times 10^{-4})\eta_{\rm acc}$ G at apastron, if the emitter is close to the compact object. Using the lower and upper limits on the magnetic field strength, an upper limit can be placed on the acceleration efficiency parameter of $\eta_{\rm acc} \lesssim 120$ at periastron and $\eta_{\rm acc} \lesssim 454$ at apastron.

Figure 3 shows the acceleration time $t_{\rm acc}$ as a function of the magnetic field strength B for different values of the accelerator efficiency parameter$\eta_{\rm acc}$, assuming an electron energy of 10 TeV. The upper limits on the magnetic field strength at periastron and apastron, which are independent of $\eta_{\rm acc}$, are marked. Two areas of the plot are shaded to indicate the allowed regions of the parameter space, corresponding to $t_{\rm acc} < 1\,{\rm day}$, $B < 0.3\,{\rm G}$, and $\eta_{\rm acc} < 120$ at periastron and $B < 0.1\,{\rm G}$ and $\eta_{\rm acc} < 454$ at apastron. The constraints are strongly dependent on the assumed location of the emitter, which has been taken to be coincident with the compact object in order to derive these limits.

Paredes-Fortuny et al. (2015) present a general pulsar wind shock scenario with an inhomogeneous stellar wind in which the B0 Ve star disc is disrupted and fragments. The resulting clumps of the disc fall into the shock region, pushing the shock closer to the pulsar. The reduction in size of the pulsar wind termination shock could allow for increased acceleration efficiency on the timescale of a few hours, depending on the size and density of the disc fragments. Such a scenario could account for the exceptionally bright TeV flares and orbit-to-orbit variations seen in LS I +61° 303.

This research is supported by grants from the U.S. Department of Energy Office of Science, the U.S. National Science Foundation and the Smithsonian Institution, and by NSERC in Canada. We acknowledge the excellent work of the technical support staff at the Fred Lawrence Whipple Observatory and at the collaborating institutions in the construction and operation of the instrument. The VERITAS Collaboration is grateful to Trevor Weekes for his seminal contributions and leadership in the field of VHE gamma-ray astrophysics, which made this study possible. A. O'FdB acknowledges support through the Young Investigators Program of the Helmholtz Association. A.W. Smith acknowledges support from the Fermi Cycle 7 Guest Investigator Program, grant number NNH13ZDA001N.

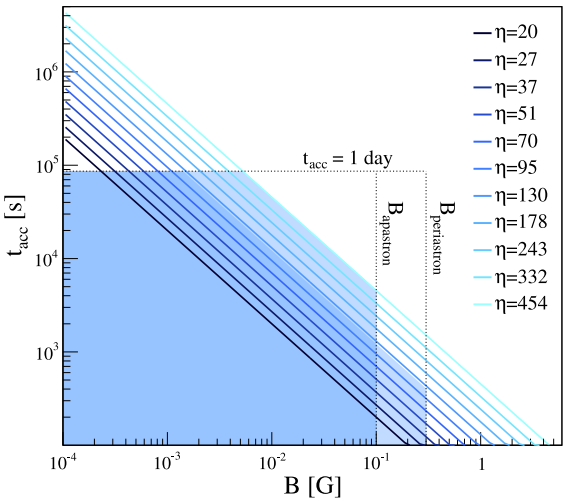

Fig. 3.— Acceleration time $t_{\rm acc}$ as a function of the magnetic field strength B for different values of the accelerator efficiency parameter $\eta_{\rm acc}$, assuming an electron energy of 10 TeV. The horizontal dotted line marks an acceleration time of one day, the maximum acceleration time of the 10 TeV electrons in the system from these observations. The vertical lines labeled $B_{\rm apastron}$ and $B_{\rm periastron}$ mark the upper limits on the magnetic field strength at apastron and periastron, respectively (these limits are independent of $\eta_{\rm acc}$). The shaded regions show the allowed regions of the parameter space for the system at apastron and periastron.

REFERENCES

Abdo, A., et al. 2009, ApJ, 701, L123

Abdo, A. A., et al. 2010, ApJ, 722, 520

Abramowski, A., Aharonian, F., Ait Benkhali, F., et al. 2015, ArXiv e-prints, arXiv:1503.02711

Acciari, V., et al. 2008, ApJ, 679, 1427

Aharonian, F., Akhperjanian, A. G., Aye, K.-M., et al. 2005a, A&A, 442, 1

—. 2005b, Science, 309, 746

Aharonian, F. A., Akhperjanian, A. G., Bazer-Bachi, A. R., et al. 2007, A&A, 469, L1

Albert, J., et al. 2006, Science, 312, 1771

Aleksic, J., et al. 2012, ApJ, 746, 80

Aliu, E., Archambault, S., Behera, B., et al. 2013, ApJ, 779, 88

Aragona, C., et al. 2009, ApJ, 698, 514

Casares, J., et al. 2005, MNRAS, 360, 1105

Dhawan, V., et al. 2006, in Proc. of Microquasars and Beyond:From Binaries to Galaxies, in Proceedings of Science, Como, IT, ed. T. Belloni, p.52

Dubus, G. 2013, A&A Rev., 21, 64

Esposito, P., Caraveo, P. A., Pellizzoni, A., et al. 2007, A&A, 474, 575

Frail, D. A., & Hjellming, R. M. 1991, AJ, 101, 2126

Holder, J. 2015, The Astronomer's Telegram, 6785

Holder, J., et al. 2008, American Institute of Physics Conference Series, 1085, 657

Hutchings, J., & Crampton, D. 1981, PASP, 93, 486

Khangulyan, D., Aharonian, F., & Bosch-Ramon, V. 2008, MNRAS, 383, 467

Kieda, D. 2013, in Proceedings of the 33rd International Cosmic Ray Conference (ICRC2013)

Li, J., et al. 2012, ApJ, 744, L13

Li, T.-P., & Ma, Y.-Q. 1983, The Astrophysical Journal, 272, 317

Lyne, A. G., Stappers, B. W., Keith, M. J., et al. 2015, MNRAS, 451, 581

Massi, M., & Jaron, F. 2013, A&A, 554, A105

Massi, M., Jaron, F., & Hovatta, T. 2015, A&A, 575, L9

Massi, M., et al. 2001, A&A, 376, 217

Paredes-Fortuny, X., Bosch-Ramon, V., Perucho, M., & Rib, M. 2015, A&A, 574, A77

Rolke, W. A., López, A. M., & Conrad, J. 2005, Nuclear Instruments and Methods in Physics Research A, 551, 493

This 2-column preprint was prepared with the AAS LaTeX macros v5.2.